

# SCIENTIFIC REPORTS



OPEN

## C10orf99 contributes to the development of psoriasis by promoting the proliferation of keratinocytes

Caifeng Chen<sup>1</sup>, Na Wu<sup>2</sup>, Qiqi Duan<sup>1</sup>, Huizi Yang<sup>3</sup>, Xin Wang<sup>1</sup>, Peiwen Yang<sup>1</sup>, Mengdi Zhang<sup>1</sup>, Jiankang Liu<sup>3</sup>, Zhi Liu<sup>4</sup>, Yongping Shao<sup>3</sup> & Yan Zheng<sup>1</sup>

Psoriasis is a chronic, relapsing inflammatory skin disease. The pathogenesis of psoriasis is complex and has not been fully understood. C10orf99 was a recently identified human antimicrobial peptide whose mRNA expression is elevated in psoriatic human skin samples. In this study, we investigated the functional roles of C10orf99 in epidermal proliferation under inflammatory condition. We showed that C10orf99 protein was significantly up-regulated in psoriatic skin samples from patients and the ortholog gene expression levels were up-regulated in imiquimod (IMQ)-induced psoriasis-like skin lesions in mice. Using M5-stimulated HaCaT cell line model of inflammation and a combinational approach of knockdown and overexpression of C10orf99, we demonstrated that C10orf99 could promote keratinocyte proliferation by facilitating the G1/S transition, and the pro-proliferation effect of C10orf99 was associated with the activation of the ERK1/2 and NF- $\kappa$ B but not the AKT pathways. Local depletion of C10orf99 by lentiviral vectors expressing C10orf99 shRNA effectively ameliorated IMQ-induced dermatitis. Taken together, these results indicate that C10orf99 plays a contributive role in psoriasis pathogenesis and may serve as a new target for psoriasis treatment.

Psoriasis is a chronic, relapsing inflammatory skin disease that affects approximately 2–3% of the world population<sup>1,2</sup>. Psoriasis is characterized by raised, sharply demarcated, erythematous plaques covered with white silvery scale. It is a lifelong disorder associated with multiple comorbidities and considerable psychosocial disability that severely impair the quality of patients' life<sup>3,4</sup>. Typical histological features of psoriatic skin include hyperkeratosis, parakeratosis, epidermal hyperproliferation, dilation of dermal capillaries and infiltration of inflammatory cells in both dermis and epidermis<sup>5–7</sup>. Although the pathogenesis of psoriasis is complex and has not been fully elucidated, accumulating evidence show that antimicrobial peptides (AMPs), such as LL37, S100 proteins and  $\beta$ -defensins, play important roles in the pathogenesis of psoriasis<sup>8–11</sup>.

C10orf99 (chromosome 10 open reading frame 99), also known as AP-57 (antimicrobial peptide with 57 amino acid residues), was recently identified as a novel human antimicrobial peptide<sup>12</sup>. However, the cellular function of C10orf99 remains largely unknown. One study reported that C10orf99 inhibits colon cancer cell growth<sup>13</sup>. Transcriptomic studies and genomic-scale analysis showed that C10orf99 mRNA is significantly elevated in psoriasis patients, and 2610528A11Rik, the mouse homolog of C10orf99, is also significantly up-regulated in psoriatic mice<sup>14–18</sup>. However, whether C10orf99 is directly involved in the pathogenesis of psoriasis has not been investigated.

In this study, our data showed that C10orf99 was significantly up-regulated in psoriatic skin samples from patients and in IMQ-induced psoriasis-like mice. C10orf99 knockdown in HaCaT cells decreased keratinocyte proliferation by inducing cell cycle arrest under psoriatic inflammation. Overexpression of C10orf99 promoted the proliferation of HaCaT cells by activating two pro-proliferative pathways: the extracellular signal-regulated

<sup>1</sup>Department of Dermatology, the Second Affiliated Hospital, School of Medicine, Xi'an Jiaotong University, Xi'an, China. <sup>2</sup>Department of Dermatology, Shaanxi Provincial People's Hospital, Xi'an, China. <sup>3</sup>Frontier of institute of science and technology and Key Laboratory of Biomedical Information Engineering of Ministry of Education, School of Life Science and Technology, Xi'an Jiaotong University, Xi'an, China. <sup>4</sup>Department of Dermatology, University of North Carolina, Chapel Hill, NC, USA. Correspondence and requests for materials should be addressed to Y.S. (email: [yongpings@gmail.com](mailto:yongpings@gmail.com)) or Y.Z. (email: [zenyan66@126.com](mailto:zenyan66@126.com))

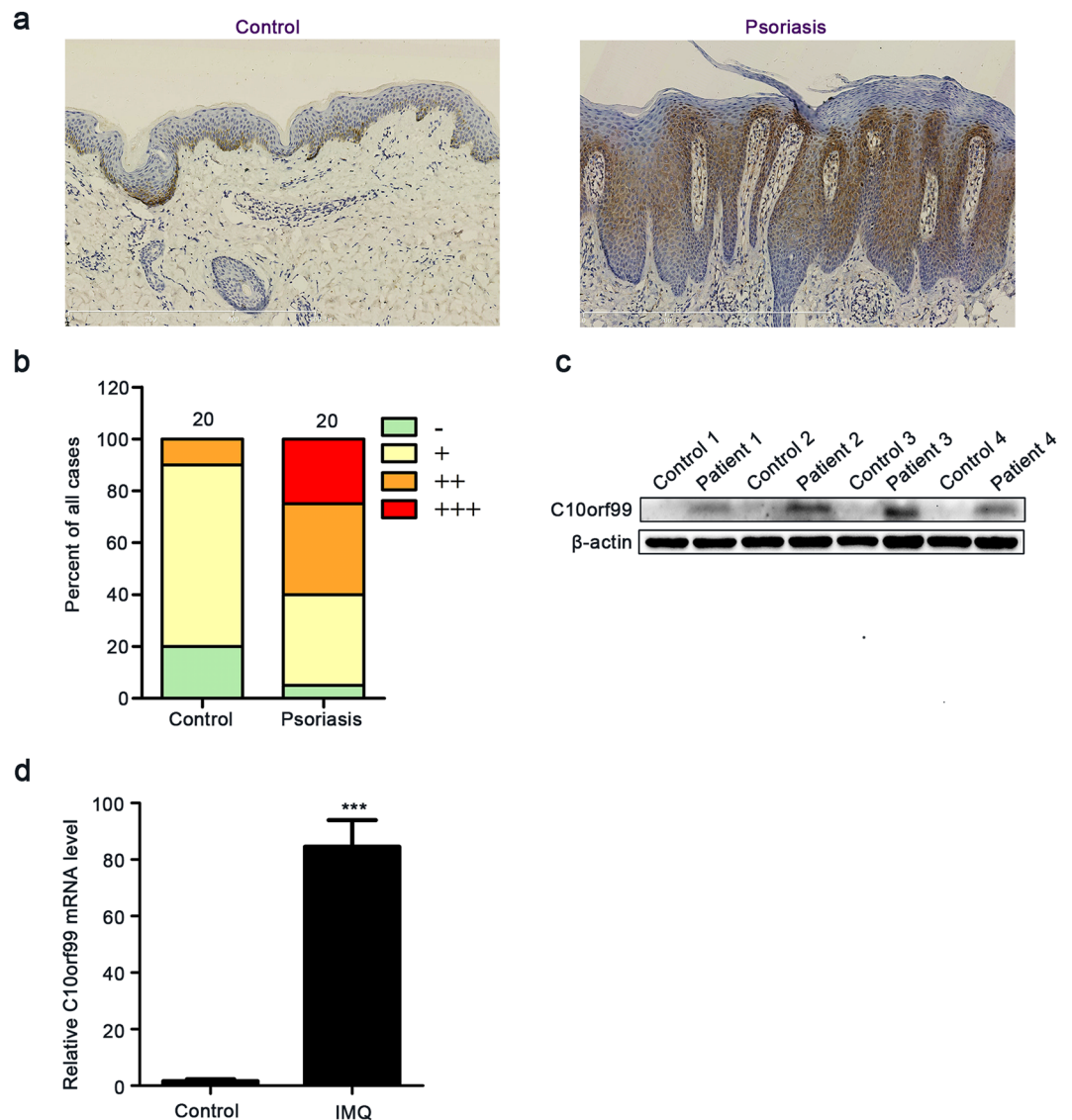


**Figure 1.** C10orf99 expression in psoriatic lesions. (a) Representative immunohistochemistry staining of healthy human skin (n = 20) and psoriatic human skin (n = 20). Bar length = 100  $\mu$ m. (b) Semiquantitative analysis of C10orf99 staining results from 20 healthy and 20 psoriatic skin samples. (c) C10orf99 expression was detected by Western blot in skin tissues from psoriasis patients (n = 4) and healthy controls (n = 4). (d) C10orf99 expression was evaluated using qRT-PCR in back skins of control (n = 6) and IMQ-induced psoriasis mice (n = 6). \*\*\* $P < 0.001$ .

kinase1/2 (ERK1/2) and NF- $\kappa$ B pathways. Blocking C10orf99 expression ameliorated epidermal hyperplasia, microangiogenesis and the infiltration of inflammatory cells in IMQ-induced psoriasis-like mice. Our results suggested that C10orf99 plays a contributive role in the pathogenesis of psoriasis and may serve as a potential therapeutic target for psoriasis.

## Results

**Expression of C10orf99 is elevated in psoriatic lesions.** We first examined the expression of C10orf99 at protein level in skin samples obtained from psoriasis patients (n = 20) and healthy donors (n = 20) using immunohistochemical analysis. Staining of C10orf99 was mostly observed in cytoplasm (Fig. 1a). C10orf99 was mainly expressed in the basal layer of the epidermis in the normal skin; however, in psoriasis skin, C10orf99 was over-expressed throughout the thickened epidermis. Semi-quantitative analysis of the immunohistochemistry results indicated that the expression of C10orf99 is remarkably elevated in psoriatic skins compared to the normal controls (Table 1 and Fig. 1b). This observation was further confirmed by comparative western blot analysis of skin samples from 4 psoriasis patients and 4 healthy donors (Fig. 1c). In addition, we analyzed the expression of the mouse homolog of C10orf99, termed 2610528A11Rik, in the IMQ-induced mouse model<sup>19</sup>. Consistently, the expression of 2610528A11Rik was also significantly increased at the mRNA level in the skin lesions from IMQ-treated mice (Fig. 1d). Taken together, these data demonstrate an overexpression of C10orf99 in the psoriatic skin lesions.

Group	Case	Expression				p-value
		negative	weakly positive	moderately positive	strong positive	
Normal skin	20	4	14	2	0	0.001**
Psoriasis skin	20	1	7	7	5	

**Table 1.** Expression of C10orf99 in Normal skin and Psoriasis. Score 0, negative; score 1–4, weakly positive; score 5–8, moderately positive; score 9–12, strong positive. \*\* $P < 0.01$ , compared to normal skin.

### C10orf99 knockdown inhibits HaCaT cell proliferation by inducing G1/S-growth arrest.

Enhanced keratinocyte proliferation is an important feature of psoriasis. Since C10orf99 regulates cell proliferation in cancer cells<sup>13</sup> and is significantly overexpressed in psoriatic skins, we determined whether C10orf99 may contribute to the development of psoriasis by regulating keratinocyte proliferation. We first tested its role in a well-established cell culture model of inflammation that recapitulates some features of psoriasis by stimulating HaCaT cells with a cocktail of cytokines M5 (including TNF- $\alpha$ , IL-17A, IL-22, IL-1 $\alpha$ , and Oncostatin-M, 10 ng/ml)<sup>20,21</sup>. As shown previously, expressions of TNF- $\alpha$ , IL-6, IL-8 and h-BD2 were markedly increased in HaCaT cells after 24 h treatment of M5 (Fig. 2a)<sup>20</sup>. More importantly, both western blot and qRT-PCR analysis showed that C10orf99 expression was greatly elevated in M5-stimulated HaCaT cells (Fig. 2a). Thus, HaCaT cells stimulated with M5 could serve as a cell culture model to investigate the role of C10orf99 in the proliferation of keratinocytes.

We then used two independent C10orf99-specific siRNAs to transiently decrease C10orf99 expression in M5-stimulated HaCaT cells. Western blot and qRT-PCR results confirmed the effective down-regulation of C10orf99 by both siRNAs (Fig. 2b). In the absence of the inflammatory cytokine cocktail M5, depletion of C10orf99 had none (siRNA-1) or very weak inhibitory effect (siRNA-2) on HaCaT cell growth (Supplementary Figure S5), presumably due to a very low basal expression level of C10orf99. Previous studies have shown that M5 treatment accelerates the growth of HaCaT cells by around 1.5 fold<sup>22,23</sup>. Notably, C10orf99 knockdown significantly reduced the growth rate of M5-stimulated HaCaT cells as demonstrated by the MTT assays (Fig. 2c). Cell cycle analysis by PI staining further revealed that C10orf99 knockdown led to a G1/S growth arrest accompanied by reduced expressions of G1-S progression regulators such as Cyclin D1 and Cyclin A (Fig. 2d,e). Thus, C10orf99 depletion inhibits the growth of keratinocytes under inflammatory conditions.

**C10orf99 downregulation has no effect on keratinocyte apoptosis.** We also assessed the effect of C10orf99 downregulation on keratinocyte apoptosis by Annexin V/PI staining. However, no significant difference in apoptosis rate was observed between C10orf99-depleted and control cells, demonstrating that C10orf99 knockdown did not affect HaCaT cell apoptosis, ruling out a possibility that the reduced growth rate in C10orf99 knockdown HaCaT cells was caused by increased apoptosis (Supplementary Figure S1).

**Overexpression of C10orf99 promotes the proliferation of HaCaT cells.** To further confirm the role of C10orf99 in the regulation of KC proliferation, we over-expressed C10orf99 via a lentiviral vector in HaCaT cells without M5 treatment, which express low basal level of C10orf99. Lentivirus-mediated expression of exogenous C10orf99 was verified by qRT-PCR and western blot analysis (Fig. 3a,b). MTT assay showed that over-expression of C10orf99 increased the proliferation of HaCaT cells as compared with the blank or the empty virus control (Fig. 3c). PI cell cycle analysis revealed that overexpression of C10orf99 resulted in an increased S phase population with a concomitant decrease in the G1/G0 phase population (Fig. 3d). As expected, the expressions of the G1/S progression regulators, Cyclin D1 and Cyclin A were increased in C10orf99 over-expressed HaCaT cells versus the control cells (Fig. 3e). Therefore, C10orf99 overexpression promotes the proliferation of HaCaT cells by facilitating the G1/S progression.

**C10orf99 activates the ERK1/2 and the NF- $\kappa$ B signaling.** We initially evaluated phospho-p65, phospho-ERK1/2 and phospho-AKT expressions in M5-treated HaCaT cells by western blot. We observed that all these pathways were prominently activated after incubation with M5 for 15 to 30 min (Fig. 4a). To study the molecular mechanisms underlying the pro-proliferation function of C10orf99, we used C10orf99-specific siRNAs to decrease the expression of C10orf99 followed by treated with M5 for 30 min and analyzed several key proteins involved in the signaling pathways. The data demonstrated that knockdown of C10orf99 suppressed the activity of ERK1/2 and NF- $\kappa$ B signaling, as evidenced by the reduction of the levels of p-ERK1/2 and p-p65, but not the AKT pathway (Fig. 4b). Conversely, over-expression of C10orf99 increased the levels of p-ERK1/2 and p-p65 (Fig. 4c). Therefore, the pro-proliferation activity of C10orf99 is associated with the activation of the ERK1/2 and NF- $\kappa$ B pathways.

**C10orf99 knockdown ameliorates imiquimod-induced dermatitis.** To determine whether C10orf99 participates in the pathogenesis of psoriasis by promoting keratinocyte proliferation, we locally knocked down C10orf99 expression in mouse back skin by injecting lentiviral particles carrying the C10orf99 shRNA and examined the impact of C10orf99 depletion on the development of IMQ-induced psoriasis<sup>24,25</sup>. The knockdown efficiencies of three shRNAs were first verified in a mouse cell line C2C12 which expresses endogenous C10orf99. Out of three shRNAs, shRNA-1 showed the best knockdown efficiency and was therefore chosen for the *in vivo* experiment (Supplementary Figure S2). The *in vivo* knockdown efficiency of shRNA-1 was confirmed by qRT-PCR analysis on skin tissues from the virus-injected area (Fig. 5a). IMQ treatment induced sharply demarcated erythematous plaques covered with white silvery scale on mouse back. However, C10orf99 knockdown led to a significant decrease in plaque formation (Fig. 5b). Histological analysis of the skin sections revealed that

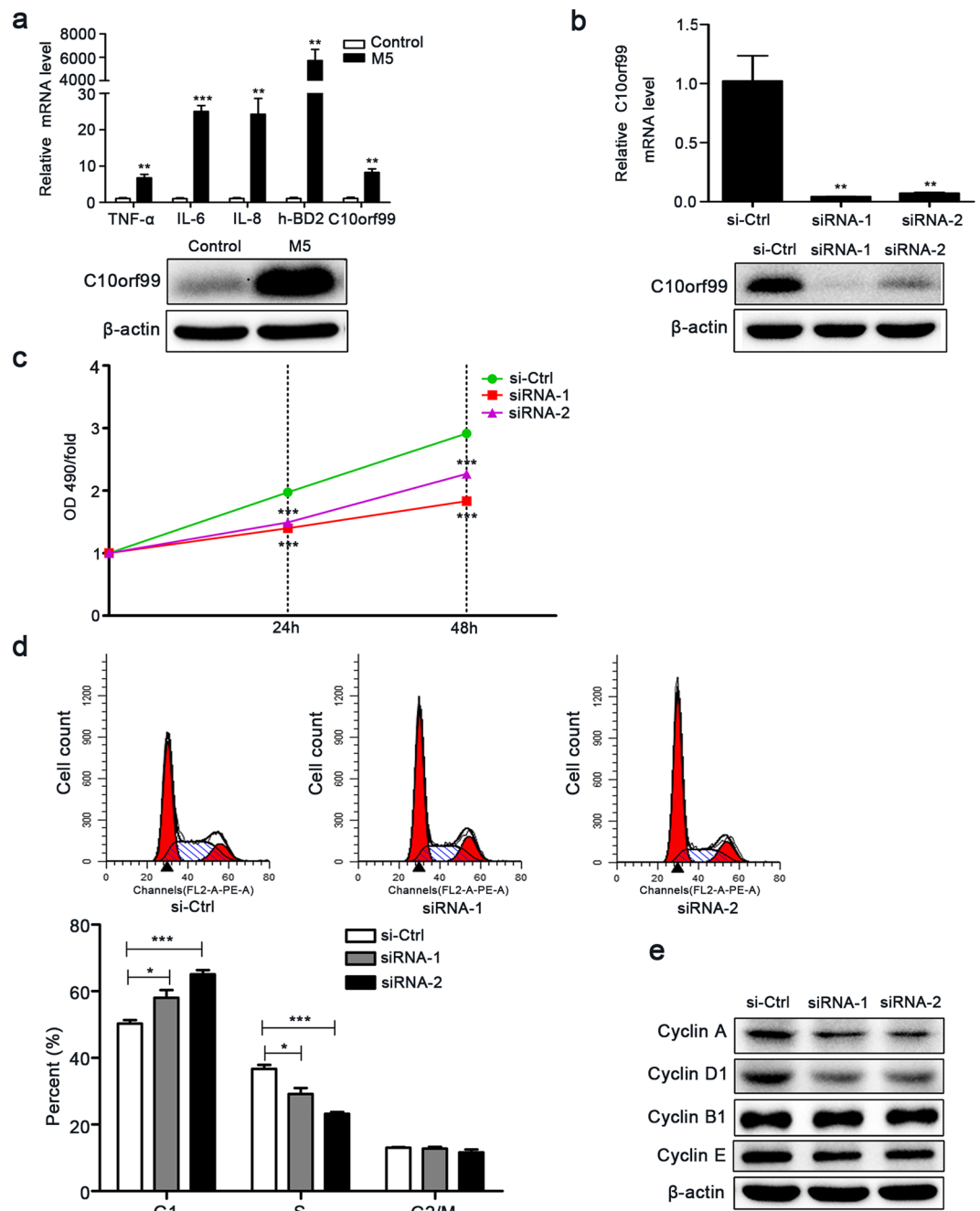


**Figure 2.** Effect of C10orf99 knockdown on cell proliferation under psoriatic inflammation. **(a)** Expression of inflammatory cytokines and C10orf99 in M5-stimulated HaCaT cells was detected by qRT-PCR (24 h after treatment) and western blot (48 h after treatment). **(b)** C10orf99 mRNA (48 h after transfection) and C10orf99 protein expression (72 h after transfection) was measured in M5-treated HaCaT cells transfected with the C10orf99 small interfering RNA (siRNA) or NC-siRNA (si-Ctrl). **(c)** MTT assays on M5-stimulated HaCaT cells transfected with si-Ctrl or C10orf99 siRNA. **(d)** Cell cycle analysis was analyzed by flow cytometry 72 h after siRNA transfection. **(e)** Cell cycle regulators were measured by western blot 72 h after siRNA transfection with  $\beta$ -actin being an internal control. The data are representative of at least three independent experiments. \* $P < 0.05$ , \*\* $P < 0.01$ , \*\*\* $P < 0.001$ . h, hours; Ctrl, control; OD, optical density; MTT, 3-(4,5-dimethylthiazol-2-yl)-2,5-diphenyltetrazolium bromide.

the epidermal hyperplasia was ameliorated, the epidermal thickness was decreased and microangiogenesis and the infiltration of inflammatory cells were reduced in C10orf99-depleted mice compared to the control mice (Fig. 5c,d). Prominent increases in p-p65, p-ERK1/2, p-AKT, Cyclin A and Cyclin D1 levels were observed after IMQ applied for 7 consecutive days (Fig. 5e). In addition, we found that C10orf99 knockdown down-regulated the expression of Cyclin D1 and the angiogenesis regulator VEGF (Fig. 5f). Moreover, consistent with the results *in vitro*, knock-down of C10orf99 by shRNA decreased the activity of ERK1/2 and NF- $\kappa$ B signaling, as

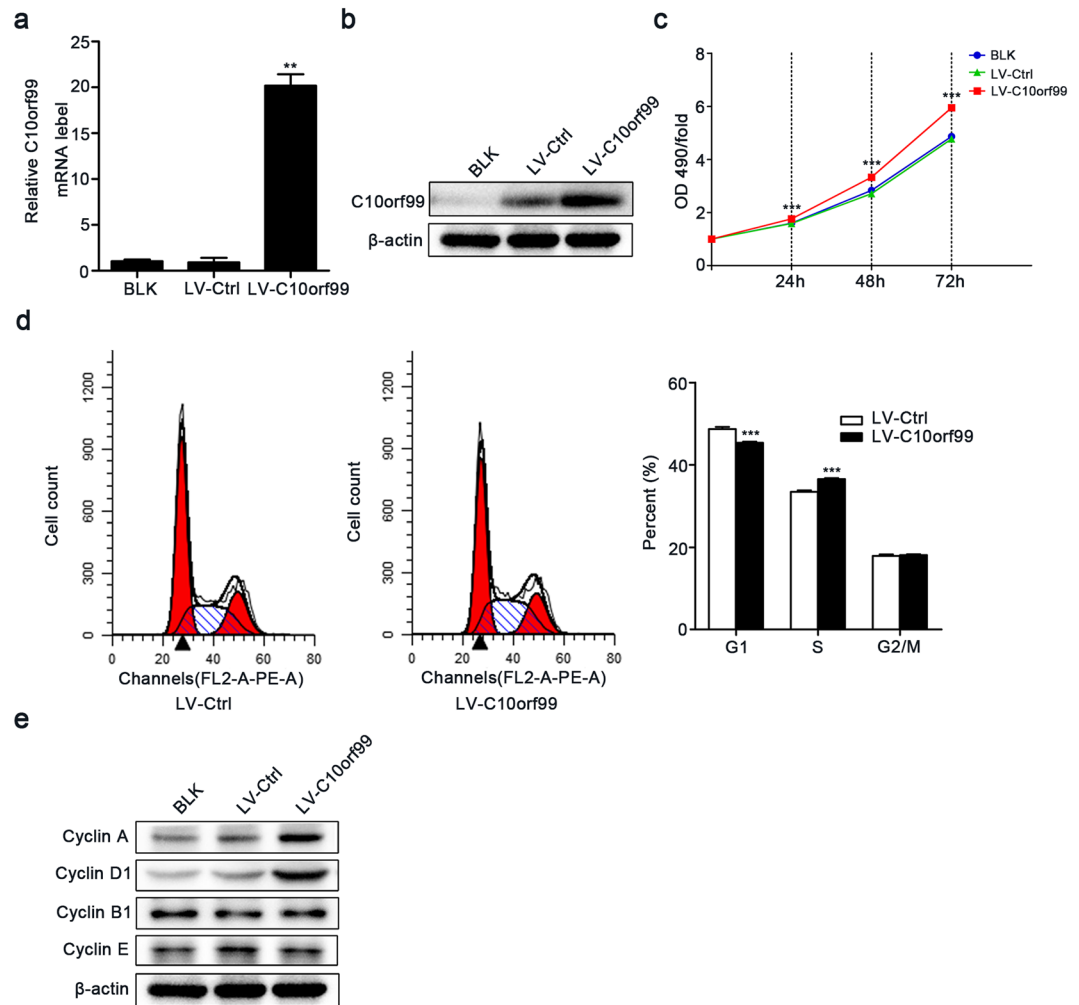


**Figure 3.** Effect of C10orf99 overexpression on cell proliferation. (a) C10orf99 mRNA and (b) protein expressions were determined after lentiviral particles transduction in HaCaT cells. (c) MTT assays on HaCaT cells transduced with control or C10orf99-expressing lentiviruses. (d) Cell cycle distribution was analyzed by flow cytometry, and the percentages of cells in different cycle phases were calculated. (e) Protein expression levels of cell cycle regulators were analyzed. Data are representative of at least three independent experiments. \*\* $P < 0.01$ , \*\*\* $P < 0.001$ . BLK, blank transfected group; LV-Ctrl, vector transfected group; LV-C10orf99, C10orf99-expressing lentiviruses transfected group.

demonstrated by downregulation of p-ERK1/2 and p-p65 (Fig. 5f). These data further supported that C10orf99 plays an important role in the development of psoriasis.

## Discussion

C10orf99 was recently identified as a new human AMP<sup>12</sup>. Its gene is located on chromosome 10q23.1 and encodes a short basic peptide of 57 amino acid residues<sup>12</sup>. It has been found that C10orf99 mRNA has distinct tissue-specific expression patterns: highly expressed in colon, moderately expressed in tonsil and almost undetectable in other tissues<sup>13</sup>. Like other AMPs, such as LL-37 and h-BD2, C10orf99 also exhibits potent wide-spectrum antimicrobial activity against bacteria, fungi and viruses<sup>12</sup>. A study of large-scale mouse knockout library screen implicated C10orf99 in the immune regulation, for C10orf99 knockout mouse exhibits a decreased serum IgM level and an increased ratio of CD4<sup>+</sup>/CD8<sup>+</sup> cells<sup>26</sup>. Similar to other AMPs, *in situ* gel-forming AP-57 peptide promotes cutaneous wound healing<sup>27–30</sup>. Recently, C10orf99 was speculated to participate in the pathogenesis of psoriasis without the support of any experimental data<sup>15</sup>. Therefore, it is of great interest to investigate the function of C10orf99 in the development of psoriasis.

In this work, we demonstrated that the expressions of C10orf99 and its ortholog were significantly up-regulated in the skin of psoriasis patients and IMQ-induced psoriatic mouse models respectively. We also showed that C10orf99 positively regulates keratinocyte proliferation. Paradoxically, C10orf99 was previously found to be growth-inhibitory in colon cancer cells<sup>13</sup>. The proliferation of keratinocyte is a complex process regulated by a variety of intracellular/extracellular agents including growth factors, neuropeptides, interleukins and inflammatory mediators, many of which may play versatile roles in different cellular/environmental contexts. It

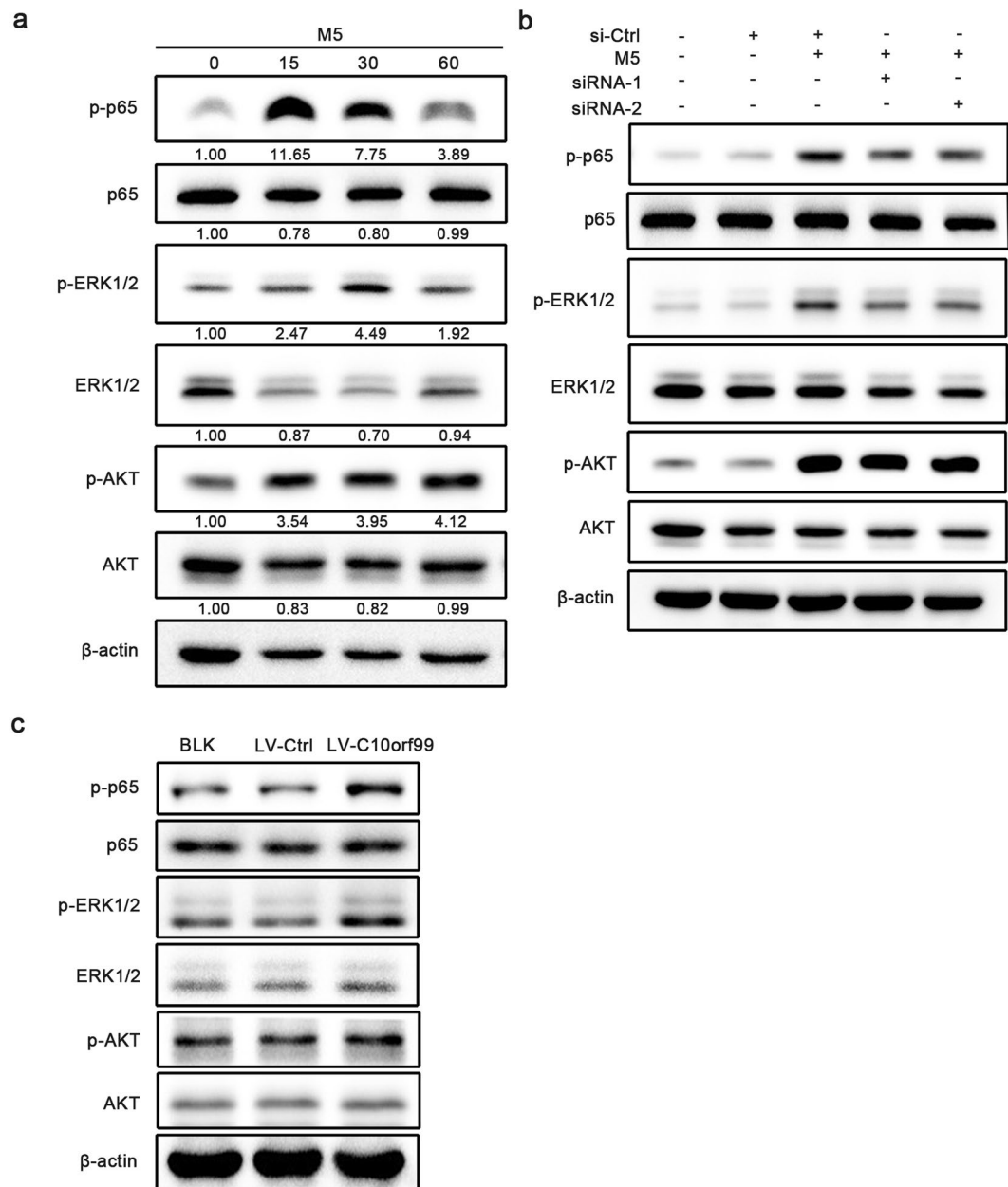


**Figure 4.** C10orf99 regulates the keratinocyte proliferation by activating ERK1/2 and NF- $\kappa$ B pathways. **(a)** HaCaT cells were treated with M5 for 15, 30 and 60 min, and the phosphorylation of NF- $\kappa$ B p65, ERK1/2 and AKT were detected by western blot. **(b)** HaCaT cells were transfected with C10orf99 siRNAs for 48 h and then incubated with M5 for 30 min. Cells were lysed for western blot analysis on indicated proteins. **(c)** Phosphorylation of NF- $\kappa$ B p65, ERK1/2 and AKT were analysed by western blot in HaCaT cells transduced with lentiviral particles.  $\beta$ -actin was used as an internal control. Data are representative of three independent experiments. Ctrl, control; BLK, blank transfected group; LV-Ctrl, vector transfected group; LV-C10orf99, C10orf99-expressing lentiviruses transfected group.

is not unusual that a protein performs opposite functions in the proliferation of two different epithelial cell lines. For instance, studies have shown that the S100A8/S100A9 complex, which has a broad range of intracellular and extracellular functions, suppresses keratinocyte proliferation, but promote the growth and metastasis of colorectal cancer cells<sup>31,32</sup>. How can the contradictory role of C10orf99 on cell proliferation be explained? The previous paper claimed that C10orf99 could inhibit colon cancer cell growth via interacting with SUSD2<sup>13</sup>. However, a transcriptome analysis demonstrated that SUSD2 was significantly down-regulated in psoriatic lesions<sup>18</sup>. In line with this, we observed that the expression of SUSD2 mRNA also decreased in M5-treated HaCaT cells (Supplementary Figure S3). Thus, it's likely that C10orf99 regulates keratinocyte proliferation through a distinct mechanism independent of the SUSD2 pathway. Furthermore, knockdown of C10orf99 in the colon cancer cell line DLD1 does not alter the ERK1/2 pathway activity (Supplementary Figure S4). Interestingly, recently studies

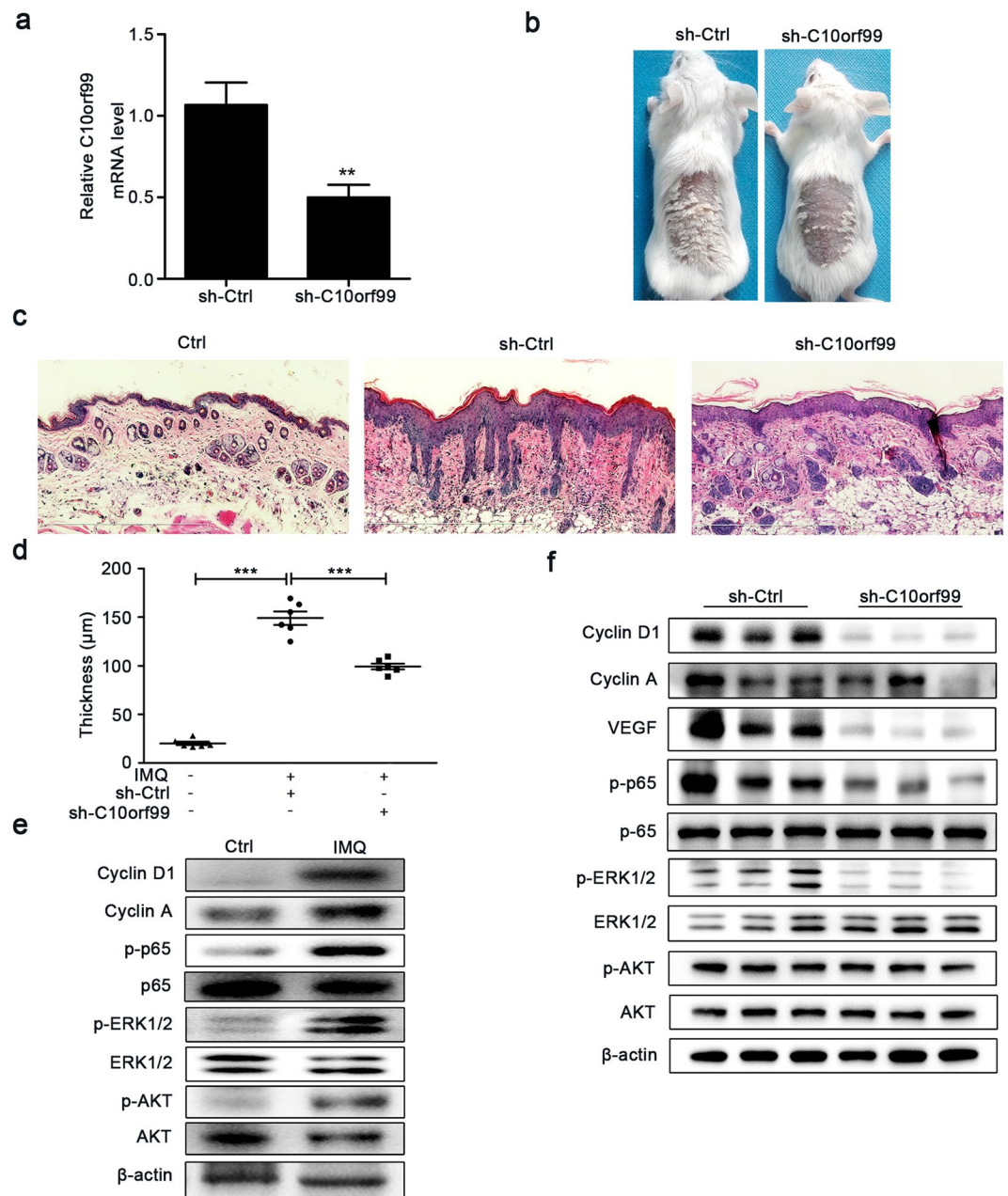


**Figure 5.** C10orf99 knockdown reduced the epidermal thickness of IMQ-induced psoriasis mouse model. **(a)** qRT-PCR analysis of mC10orf99 expression in the back skins of mice infected with the lentiviruses and treated with IMQ (7 days). **(b)** Phenotypic presentation of the back skins of mice after lentivirus infection and IMQ treatment for 7 days. **(c)** Representative histological sections of the back skins of control (Ctrl) (n = 6) or IMQ-induced psoriatic mice injected intradermally with C10orf99 shRNA (sh-C10orf99) (n = 6) or negative control shRNA (sh-Ctrl) (n = 6) examined by hematoxylin and eosin staining. Bar = 600 μm. **(d)** Epidermal thickness of the mouse back skins was measured. Each point represents one mouse skin sample. **(e)** Western blot analysis of Cyclin A, Cyclin D1, NF-κB p65, phosphorylation of NF-κB p65, AKT, ERK1/2 in skin tissues from control and IMQ-induced psoriatic mice. **(f)** Western blot analysis of Cyclin A, Cyclin D1, VEGF and phosphorylation of NF-κB p65, AKT, ERK1/2 in skin tissues from IMQ-induced psoriatic mice injected intradermally with lentiviruses. β-actin was used as an internal control. Data are representative of three independent experiments. \*\* $P < 0.01$ , \*\*\* $P < 0.001$ .

found that C10orf99 is a natural ligand for the orphan receptor GPR15<sup>33,34</sup>. We speculated that, like other AMPs and chemokines, C10orf99 may function through different receptor pathways in different cellular contexts and exert versatile impacts on the proliferation of cells.

AKT, ERK1/2 and NF-κB signaling pathways play important roles in many biological functions. Studies have shown that the expression of all these protein kinases were significantly elevated in psoriatic skin and they play critical roles in the pathogenesis of psoriasis<sup>35–39</sup>. Our results *in vitro* showed that M5 greatly activated the AKT,

ERK1/2 and NF- $\kappa$ B signaling pathways. C10orf99 signaling was previously speculated to involve the AKT pathway. Interestingly, our data showed that knockdown of C10orf99 decreased the level of p-ERK1/2, but not p-AKT, in the cell culture model of psoriasis. In addition, C10orf99 knockdown resulted in a significant reduction of p-p65, indicative of the down-regulation of the NF- $\kappa$ B pathway activity. Conversely, over-expression of C10orf99 promoted the activity of ERK pathway and NF- $\kappa$ B pathway. Thus, C10orf99 likely regulates the proliferation of keratinocyte by activating the ERK1/2 and the NF- $\kappa$ B signaling.

The regulatory role of C10orf99 in keratinocyte proliferation *in vitro* prompted us to assess its functionality *in vivo*. The IMQ-induced psoriasis-like mouse model recapitulates many features of human psoriasis and has been widely used to study the disease pathology. In the IMQ-treated mice, C10orf99 knockdown attenuated epidermal hyperproliferation, infiltration of inflammatory cells and microangiogenesis, which was accompanied by the decreased expression of VEGF. C10orf99 knockdown also decreased the expression of Cyclin D1, p-ERK1/2 and p-p65. However, the knockdown of C10orf99 had marginal effects on Cyclin A, which likely due to different cellular environments between *in vitro* and *in vivo*.

In summary, our results show that C10orf99 protein is highly expressed in psoriatic skin and that it regulates keratinocyte proliferation likely through activation of the ERK1/2 and NF- $\kappa$ B pathway. Furthermore, downregulation of C10orf99 ameliorates IMQ-induced psoriasis in mice. Thus, C10orf99 has a contributive role in psoriasis pathogenesis and may be a new target for psoriasis treatment.

## Materials and Methods

**Human skin tissue collection.** A total of 40 paraffin-embedded tissues including 20 psoriasis tissues (11 male and 9 female, age range = 7–50 years) and 20 normal skin tissues (10 male and 10 female, age range = 10–43 years) for IHC were obtained from the tissue bank of the Department of Dermatology at the Second Affiliated Hospital of Xi'an Jiaotong University. In addition, we collected 8 fresh tissue samples including 4 psoriasis samples and 4 normal samples by punch biopsy under local lidocaine anaesthesia for Western blotting. The fresh tissue samples were snap frozen in liquid nitrogen and stored at  $-80^{\circ}\text{C}$ . Written informed consents were obtained from all patients. The study was performed in accordance with the declaration of Helsinki Principles and approved by the Research Ethics Board of the Second Affiliated Hospital of Xi'an Jiaotong University. All of the specimens were pathologically confirmed.

**Immunohistochemistry.** Immunohistochemistry was performed according to standard methods. The IHC results were scored independently by three experienced pathologists under microscope and quantified based on the following scoring system in a semiquantitative manner as previously reported<sup>40,41</sup>. The rate of positively stained cells was scored as follows: 0 ( $\leq 5\%$ ), 1 (6–25%), 2 (26–50%), 3 (51–75%), 4 ( $> 75\%$ ). The staining intensity was graded as follows: 0 (colorless), 1 (light yellow), 2 (yellowish brown), 3 (chocolate brown). The score for each microscopic field was calculated by multiplying the two scores. The average score of five fields was taken as the final immunoreactivity score.

**Histological analysis.** The mouse back skin was collected, fixed in formalin and embedded in paraffin. Sections were stained with haematoxylin and eosin. Epidermal hyperplasia (acanthosis) was quantified by measuring its thickness as described previously<sup>42</sup>. Firstly, Hamamatsu digital pathology system was used to scan the HE-stained sections. Then, the NDP.view software was used to evaluate the epidermis thickness and it measured the distance from the basal lamina to the bottom of the stratum corneum in HE-stained skin sections. Eight randomly-chosen fields of each section were measured and the mean was calculated.

**Cell culture.** HaCaT cells (an immortalized human keratinocyte cell line), C2C12 cells (mouse muscle cell line) and DLD1 cells were cultured in Dulbecco's modified Eagle's medium supplemented with 10% fetal bovine serum and 1% penicillin/streptomycin at  $37^{\circ}\text{C}$  in a humidified atmosphere with 5%  $\text{CO}_2$ .

**Induction of psoriatic model *in vitro*.** HaCaT cells were stimulated with a cocktail of cytokines, M5, which includes TNF- $\alpha$ , IL-17A, IL-22, IL-1 $\alpha$ , and Oncostatin-M (Peprotech, USA) to induce psoriatic inflammation<sup>20,21</sup>.

**siRNA transfection.** The siRNAs for C10orf99 and a nonsilencing-siRNA used as the negative control were synthesized by GenePharma (Shanghai, China) and the sequences were listed in Supplementary Table S1. The siRNAs were transiently transfected into cells using Lipofectamine RNAiMAX (Invitrogen) according to the manufacturer's instructions. After 24 h for transfection, M5 was added to stimulate the transfected cells.

**Lentivirus transduction.** The C10orf99-overexpressing lentivirus particles were purchased from GenePharma (Shanghai, China). Cells were incubated with 100  $\mu\text{l}$  of the virus suspension (titer  $1 \times 10^8$  TU/ml) for 48 h and selected with puromycin (5 mg/ml) in the culture medium for 2 weeks.

**3-(4,5-dimethylthiazol-2-yl)-2,5-diphenyltetrazolium bromide (MTT) assay.** 4000 transfected cells per well were plated in 96-well plate, which were then incubated at  $37^{\circ}\text{C}$ , 5%  $\text{CO}_2$ . At the indicated time points, 10% volume of MTT solution (5 mg/ml) was added to each well and incubated at  $37^{\circ}\text{C}$  for 4 h. Then 200  $\mu\text{l}$  dimethylsulfoxide was added to dissolve the formazan crystals after removing the medium. Optical density (OD) value was measured at 490 nm wavelength.

**PI cell cycle analysis.** Cells were harvested and fixed in cold 70% ethanol at  $-20^{\circ}\text{C}$  overnight. For the analysis, PI staining solution (50 mg/mL PI and 100 mg/mL ribonuclease A) was added to the cells and incubated at  $37^{\circ}\text{C}$  for 30 minutes in dark. Cell cycle was analyzed using flow cytometry (FACSCalibur from BD Biosciences, USA).



**Annexin V/PI staining.** Cells were harvested by trypsinization without ethylenediaminetetraacetic acid (EDTA). The cells then were suspended by 500  $\mu$ l binding buffer and incubated with 5  $\mu$ l Annexin V-FITC (fluorescein isothiocyanate) solution and 5  $\mu$ l Propidium Iodidum for 15 min at room temperature in dark. Flow cytometry was used to analyze cell apoptosis.

**RNA extraction and Quantitative Real-Time PCR.** Total RNA was extracted from skin samples or HaCaT cells using Trizol reagent (Invitrogen). Quantitative realtime PCR (qRT-PCR) was performed on a real-time PCR system (Eppendorf, Germany) using SYBR Green Premix Ex Taq (TaKaRa, Dalian, China). Primers were synthesized by Baiaoke Biotech (Beijing, China) and the following primers were used: human GAPDH: forward 5'-TGTTGCCATCAATGACCCCTT-3', and reverse 5'-CTCCACGACGTACTCAGCG-3'; human C10orf99: forward 5'-GCTTCTCTGCTTCTCCATCTTCT-3', and reverse 5'-TTCAGGTTTGTGAGTTGGG-3'; human TNF- $\alpha$ : forward 5'-TCCTTCAGACACCCTCAACC-3'; and reverse 5'-AGGCCCCAGTTTGAATTCTT-3'; human IL-6: forward 5'-AAGCCAGAGCTGTGCAGATGAGTA-3', and reverse 5'-TGTCTGCAGCCACTGGTTC-3'; human IL-8: forward 5'-GTCCTTGTTCCTACTGTGCCT-3', and reverse 5'-GCTTCCACATGTCCTCACAA-3'; human BD2: forward 5'-TCAGCCATGAGGGTCTTGTA-3', and reverse 5'-GGATCGCCTATACCACCAAAA-3'; mouse 2610528A11Rik: forward 5'-TTCTAGCCCTTTCCGGTCTG-3', and reverse 5'-CACCACCCATGACTTGACTG-3'; mouse  $\beta$ -actin: forward 5'-CCTCTATGCCAACACAGTGC-3', and reverse 5'-ACATCTGCTGGAAGGTGGAC-3'. GAPDH or  $\beta$ -actin was used as internal controls. The relative quantification of gene was obtained using the  $2^{-\Delta\Delta CT}$  method relative to the internal control.

**Western blot.** Total protein was prepared from cells or skin samples using RIPA lysis buffer containing 1 mM PMSF and the protein was quantified by BCA protein assay. The prepared proteins (15  $\mu$ g) were separated by 10–12% SDS-PAGE and transferred to nitrocellulose membrane or polyvinylidene difluoride membrane. The membrane was blocked with TBST containing 5% skim milk for 1 h at room temperature and incubated with the primary antibodies at 4 °C overnight. The following primary antibodies were used: Cyclin A (sc-596), Cyclin B1 (sc-595), Cyclin D1 (sc-246), Cyclin E (sc-25303), NF- $\kappa$ B p65 (sc-71675), p-NF- $\kappa$ B p65 (#3033), AKT (#9272 s), p-AKT (#4051 s), ERK1/2 (#9102), p-ERK (#3192 s), VEGF (sc-7269),  $\beta$ -actin (60008–1-Ig), C10orf99 (ab151109). The membrane was then incubated in horseradish peroxidase-conjugated goat anti-mouse or anti-rabbit secondary antibodies at room temperature for 1 h. ECL kit (Pierce Chemical, Rockford, IL, USA) was used to perform chemiluminent detection.

**Mice.** Eight-week-old female BALB/c mice were purchased from the Animal Experiment Center of Xi'an Jiaotong University and they were kept under a 12 h light/dark cycle with specific pathogen-free conditions. All mice were housed at least 1 week prior to the study and provided with food and purified water ad libitum. All procedures involved in mice were performed in compliance with the Animal Care and Use Committee guidelines of Xi'an Jiaotong University School of Medicine.

**IMQ-induced mouse model of psoriasis.** Mice were anesthetized with 200  $\mu$ l 0.6% sodium pentobarbital and their backs were shaved with an electric clipper, then the mice were applied with a daily topical dose of 62.5 mg 5% IMQ cream (Mingxin, Chengdu, China) or Vaseline cream on their shaved back for 7 consecutive days. In the end, all mice were sacrificed. Back skin was isolated and half was fixed in 10% formaldehyde and the other half of the skin sample was finely chopped for RNA isolation and qRT-PCR analysis.

**In vivo administration of C10orf99 shRNA lentivirus.** Lentiviruses of C10orf99 shRNAs and control shRNAs were from GenePharma (Shanghai, China) and all the oligonucleotides were listed in supplementary Table S2. shRNA-1 successfully knocked down the C10orf99 mRNA expression level and was used in animal experiment. Lentivirus particles ( $1.0 \times 10^9$  TU, 50  $\mu$ L) encoding C10orf99 shRNA or negative control shRNA were injected intradermally into the shaved dorsal skin of mice. After three days, the mice started to be treated with IMQ as described above.

**Statistical analysis.** SPSS standard version 21.0 software (SPSS Inc, Chicago, IL) and GraphPad Prism 5.0 (La Jolla, CA, USA) were used for statistical analysis. Data were presented as mean  $\pm$  SEM. The Mann–Whitney U test was used for immunohistochemistry analysis and the Student's t-test was used for comparisons between two groups.  $P < 0.05$  was considered statistically significant.

**Data availability.** All data generated or analysed during this study are included in this published article (and its Supplementary Information files).

## References

- Nestle, F. O., Kaplan, D. H. & Barker, J. Psoriasis. *The New England journal of medicine* **361**, 496–509, <https://doi.org/10.1056/NEJMr0804595> (2009).
- Lowes, M. A., Bowcock, A. M. & Krueger, J. G. Pathogenesis and therapy of psoriasis. *Nature* **445**, 866–873, <https://doi.org/10.1038/nature05663> (2007).
- Langan, S. M. *et al.* Prevalence of metabolic syndrome in patients with psoriasis: a population-based study in the United Kingdom. *J Invest Dermatol* **132**, 556–562, <https://doi.org/10.1038/jid.2011.365> (2012).
- Gelfand, J. M. & Yeung, H. Metabolic syndrome in patients with psoriatic disease. *J Rheumatol Suppl* **89**, 24–28, <https://doi.org/10.3899/jrheum.120237> (2012).
- Sabat, R. *et al.* Immunopathogenesis of psoriasis. *Exp Dermatol* **16**, 779–798, <https://doi.org/10.1111/j.1600-0625.2007.00629.x> (2007).
- Raychaudhuri, S. K., Maverakis, E. & Raychaudhuri, S. P. Diagnosis and classification of psoriasis. *Autoimmun Rev* **13**, 490–495, <https://doi.org/10.1016/j.autrev.2014.01.008> (2014).

7. Griffiths, C. E. & Barker, J. N. Pathogenesis and clinical features of psoriasis. *Lancet* **370**, 263–271, [https://doi.org/10.1016/S0140-6736\(07\)61128-3](https://doi.org/10.1016/S0140-6736(07)61128-3) (2007).
8. Batycka-Baran, A., Maj, J., Wolf, R. & Szepletowski, J. C. The new insight into the role of antimicrobial proteins-alarmins in the immunopathogenesis of psoriasis. *J Immunol Res* **2014**, 628289, <https://doi.org/10.1155/2014/628289> (2014).
9. Lande, R. *et al.* Cationic antimicrobial peptides in psoriatic skin cooperate to break innate tolerance to self-DNA. *Eur J Immunol* **45**, 203–213, <https://doi.org/10.1002/eji.201344277> (2015).
10. Harden, J. L., Krueger, J. G. & Bowcock, A. M. The immunogenetics of Psoriasis: A comprehensive review. *J Autoimmun* **64**, 66–73, <https://doi.org/10.1016/j.jaut.2015.07.008> (2015).
11. Mahil, S. K., Capon, F. & Barker, J. N. Update on psoriasis immunopathogenesis and targeted immunotherapy. *Semin Immunopathol* **38**, 11–27, <https://doi.org/10.1007/s00281-015-0539-8> (2016).
12. Yang, M. *et al.* AP-57/C10orf99 is a new type of multifunctional antimicrobial peptide. *Biochem Biophys Res Commun* **457**, 347–352, <https://doi.org/10.1016/j.bbrc.2014.12.115> (2015).
13. Pan, W. *et al.* CSBF/C10orf99, a novel potential cytokine, inhibits colon cancer cell growth through inducing G1 arrest. *Sci Rep* **4**, 6812, <https://doi.org/10.1038/srep06812> (2014).
14. Nair, R. P. *et al.* Genome-wide scan reveals association of psoriasis with IL-23 and NF-kappaB pathways. *Nat Genet* **41**, 199–204, <https://doi.org/10.1038/ng.311> (2009).
15. Guo, P. *et al.* Gene expression profile based classification models of psoriasis. *Genomics* **103**, 48–55, <https://doi.org/10.1016/j.ygeno.2013.11.001> (2014).
16. Swindell, W. R. *et al.* Genome-wide expression profiling of five mouse models identifies similarities and differences with human psoriasis. *PLoS One* **6**, e18266, <https://doi.org/10.1371/journal.pone.0018266> (2011).
17. Gudjonsson, J. E. *et al.* Assessment of the psoriatic transcriptome in a large sample: additional regulated genes and comparisons with *in vitro* models. *J Invest Dermatol* **130**, 1829–1840, <https://doi.org/10.1038/jid.2010.36> (2010).
18. Li, B. *et al.* Transcriptome analysis of psoriasis in a large case-control sample: RNA-seq provides insights into disease mechanisms. *J Invest Dermatol* **134**, 1828–1838, <https://doi.org/10.1038/jid.2014.28> (2014).
19. van der Fits, L. *et al.* Imiquimod-induced psoriasis-like skin inflammation in mice is mediated via the IL-23/IL-17 axis. *J Immunol* **182**, 5836–5845, <https://doi.org/10.4049/jimmunol.0802999> (2009).
20. Guilloteau, K. *et al.* Skin Inflammation Induced by the Synergistic Action of IL-17A, IL-22, Oncostatin M, IL-1{alpha}, and TNF- $\alpha$  Recapitulates Some Features of Psoriasis. *J Immunol*, <https://doi.org/10.4049/jimmunol.0902464> (2010).
21. Teng, X. *et al.* IL-37 ameliorates the inflammatory process in psoriasis by suppressing proinflammatory cytokine production. *J Immunol* **192**, 1815–1823, <https://doi.org/10.4049/jimmunol.1300047> (2014).
22. Cheng, H. *et al.* TWEAK/Fn14 activation induces keratinocyte proliferation under psoriatic inflammation. *Exp Dermatol* **25**, 32–7, <https://doi.org/10.1111/exd.12820> (2016).
23. An, J. *et al.* Amentoflavone protects against psoriasis-like skin lesion through suppression of NF- $\kappa$ B-mediated inflammation and keratinocyte proliferation. *Mol Cell Biochem* **413**, 87–95, <https://doi.org/10.1007/s11010-015-2641-6> (2016).
24. Sun, Y. *et al.* CCN1, a Pro-Inflammatory Factor, Aggravates Psoriasis Skin Lesions by Promoting Keratinocyte Activation. *J Invest Dermatol* **135**, 2666–2675, <https://doi.org/10.1038/jid.2015.231> (2015).
25. Raoul, C. *et al.* Lentiviral-mediated silencing of SOD1 through RNA interference retards disease onset and progression in a mouse model of ALS. *Nat Med* **11**, 423–428, <https://doi.org/10.1038/nm1207> (2005).
26. Tang, T. *et al.* A mouse knockout library for secreted and transmembrane proteins. *Nat Biotechnol* **28**, 749–755, <https://doi.org/10.1038/nbt.1644> (2010).
27. Hirsch, T. *et al.* Human beta-defensin-3 promotes wound healing in infected diabetic wounds. *J Gene Med* **11**, 220–228, <https://doi.org/10.1002/jgm.1287> (2009).
28. Carretero, M. *et al.* *In vitro* and *in vivo* wound healing-promoting activities of human cathelicidin LL-37. *J Invest Dermatol* **128**, 223–236, <https://doi.org/10.1038/sj.jid.5701043> (2008).
29. Li, X. *et al.* *In situ* gel-forming AP-57 peptide delivery system for cutaneous wound healing. *Int J Pharm* **495**, 560–571, <https://doi.org/10.1016/j.ijpharm.2015.09.005> (2015).
30. Chereddy, K. K. *et al.* PLGA nanoparticles loaded with host defense peptide LL37 promote wound healing. *J Control Release* **194**, 138–147, <https://doi.org/10.1016/j.jconrel.2014.08.016> (2014).
31. Bresnick, A. R., Weber, D. J. & Zimmer, D. B. S100 proteins in cancer. *Nat Rev Cancer* **15**, 96–109, <https://doi.org/10.1038/nrc3893> (2015).
32. Bertheloot, D. & Latz, E. HMGB1, IL-1 $\alpha$ , IL-33 and S100 proteins: dual-function alarmins. *Cell Mol Immunol* **14**, 43–64, <https://doi.org/10.1038/cmi.2016.34> (2017).
33. Ocon, B. *et al.* A Mucosal and Cutaneous Chemokine Ligand for the Lymphocyte Chemoattractant Receptor GPR15. *Front Immunol* **8**, 1111, <https://doi.org/10.3389/fimmu.2017.01111> (2017).
34. Suply, T. *et al.* A natural ligand for the orphan receptor GPR15 modulates lymphocyte recruitment to epithelia. *Sci Signal* **10**, <https://doi.org/10.1126/scisignal.aal0180> (2017).
35. Johansen, C. *et al.* The mitogen-activated protein kinases p38 and ERK1/2 are increased in lesional psoriatic skin. *Br J Dermatol* **152**, 37–42, <https://doi.org/10.1111/j.1365-2133.2004.06304.x> (2005).
36. Yu, X. J. *et al.* Expression and localization of the activated mitogen-activated protein kinase in lesional psoriatic skin. *Exp Mol Pathol* **83**, 413–418, <https://doi.org/10.1016/j.yexmp.2007.05.002> (2007).
37. Samatar, A. A. & Poulikakos, P. I. Targeting RAS-ERK signalling in cancer: promises and challenges. *Nat Rev Drug Discov* **13**, 928–942, <https://doi.org/10.1038/nrd4281> (2014).
38. Risso, G., Blaustein, M., Pozzi, B., Mammi, P. & Srebrow, A. Akt/PKB: one kinase, many modifications. *Biochem J* **468**, 203–214, <https://doi.org/10.1042/BJ20150041> (2015).
39. Goldminz, A. M., Au, S. C., Kim, N., Gottlieb, A. B. & Lizzul, P. F. NF-kappaB: an essential transcription factor in psoriasis. *J Dermatol Sci* **69**, 89–94, <https://doi.org/10.1016/j.jdermsci.2012.11.002> (2013).
40. Chen, W. *et al.* Decreased expression of IL-27 in moderate-to-severe psoriasis and its anti-inflammation role in imiquimod-induced psoriasis-like mouse model. *J Dermatol Sci* **85**, 115–123, <https://doi.org/10.1016/j.jdermsci.2016.11.011> (2017).
41. Jia, J. *et al.* Yes-Associated Protein Contributes to the Development of Human Cutaneous Squamous Cell Carcinoma via Activation of RAS. *J Invest Dermatol* **136**, 1267–1277, <https://doi.org/10.1016/j.jid.2016.02.005> (2016).
42. Hsieh, W. L. *et al.* IFI27, a novel epidermal growth factor-stabilized protein, is functionally involved in proliferation and cell cycling of human epidermal keratinocytes. *Cell Prolif* **48**, 187–197, <https://doi.org/10.1111/cpr.12168> (2015).

## Acknowledgements

This work was supported by National Natural Science Foundation of China (81573055, 81773328), the Fundamental Research Funds for the Central Universities and for Changjiang Scholars, and Innovative Research Team in University (PCSIRT:1171) and partially supported by Funds of Shaanxi Province (2015KTCL03-10) and 2nd Hospital of Xi'an Jiaotong University.

### Author Contributions

Yan Zheng and Yongping Shao conceived and designed the experiment; Caifeng Chen, Na Wu, Qiqi Duan and Huizi Yang performed the experiment; Peiwen Yang and Mengdi Zhang helped analysed the results; Caifeng Chen wrote the main manuscript text; Jiankang Liu and Zhi Liu revised the manuscript. All authors reviewed the manuscript.

### Additional Information

**Supplementary information** accompanies this paper at <https://doi.org/10.1038/s41598-018-26996-z>.

**Competing Interests:** The authors declare no competing interests.

**Publisher's note:** Springer Nature remains neutral with regard to jurisdictional claims in published maps and institutional affiliations.



**Open Access** This article is licensed under a Creative Commons Attribution 4.0 International License, which permits use, sharing, adaptation, distribution and reproduction in any medium or format, as long as you give appropriate credit to the original author(s) and the source, provide a link to the Creative Commons license, and indicate if changes were made. The images or other third party material in this article are included in the article's Creative Commons license, unless indicated otherwise in a credit line to the material. If material is not included in the article's Creative Commons license and your intended use is not permitted by statutory regulation or exceeds the permitted use, you will need to obtain permission directly from the copyright holder. To view a copy of this license, visit <http://creativecommons.org/licenses/by/4.0/>.

© The Author(s) 2018